HHS Public Access

Author manuscript

Arthritis Rheumatol. Author manuscript; available in PMC 2019 April 01.

Published in final edited form as:

Arthritis Rheumatol. 2018 April ; 70(4): 566–577. doi:10.1002/art.40399.

INCREASED EXPRESSION AND MODULATED REGULATORY ACTIVITY OF CO-INHIBITORY RECEPTORS PD-1, TIGIT AND TIM-3 IN LYMPHOCYTES OF SYSTEMIC SCLEROSIS PATIENTS

Michelle Fleury, BS[1,2], **Anna C. Belkina, MD, PhD**[2,3], **Elizabeth A. Proctor, PhD**[4], **Christopher Zammitti, BS**[1], **Robert W. Simms, MD**[1], **Douglas A. Lauffenburger, PhD**[4], **Jennifer E. Snyder-Cappione, PhD**[2,3], **Robert Lafyatis, MD**[1,5], and **Hans Dooms, PhD**[1,2]

[1]Arthritis Center/Rheumatology Section, Department of Medicine, Boston University School of Medicine, Boston, MA

[2]Department of Microbiology, Boston University School of Medicine, Boston, MA

[3]Flow Cytometry Core Facility, Boston University School of Medicine, Boston, MA

[4]Department of Biological Engineering, Massachusetts Institute of Technology, Cambridge, MA

[5]Division of Rheumatology and Clinical Immunology, Department of Medicine, University of Pittsburgh, Pittsburgh, PA

Abstract

Objective—Immune dysfunction is an important component of the disease process underlying Systemic Sclerosis (SSc), but the mechanisms contributing to altered immune cell function in SSc remain poorly defined. Here, we measured the expression and function of the co-inhibitory receptors (co-IRs) PD-1, TIGIT, TIM-3, and LAG-3 in lymphocyte subsets from the peripheral blood of SSc patients.

Methods—Co-IR expression levels on immune cell subsets were analyzed using a 16-color flow cytometry panel. The functional role of co-IRs was determined by measuring cytokine production after in vitro stimulation of PBMCs in the presence of co-IR-blocking antibodies. Supernatants from PBMC stimulation cultures were added to SSc fibroblasts and their impact on fibroblast gene expression measured. Mathematical modeling was used to reveal differences between co-IR functions in SSc patients and healthy controls.

Results—The co-IRs PD-1 and TIGIT were increased, and co-expressed, in distinct T cell subsets from SSc patients, compared to healthy controls. TIM-3 was increased in SSc NK cells. PD-1, TIGIT and TIM-3 antibody blockade revealed patient-specific roles in modulating activation-induced T cell cytokine production. In contrast to healthy subjects, blocking TIGIT and TIM-3, but not PD-1, failed to reverse inhibited cytokine production in SSc patients, indicating the

Address correspondence to: Hans Dooms, PhD, Boston University School of Medicine, Arthritis Center/Rheumatology Section, 72 East Concord Street, E519, Boston, MA 02118, T: 617-414-2506; F: 617-638-5226; hdooms@bu.edu.
PROF. HANS DOOMS (Orcid ID : 0000-0001-7964-0876)

Conflict of interest: None of the authors has financial interests related to this work.

presence of enhanced T cell exhaustion in SSc. Finally, cytokines secreted in anti-TIM-3-treated PBMC cultures distinctly changed gene expression in SSc fibroblasts.

Conclusions—Altered expression and regulatory capacity of co-IRs in SSc lymphocytes may contribute to disease pathophysiology by modulating the cytokine-mediated crosstalk of immune cells and fibroblasts at inflammatory and/or fibrotic sites.

INTRODUCTION

Systemic Sclerosis (SSc) is an autoimmune connective tissue disorder causing external skin thickening that can progress to internal organ fibrosis in the presence of immune abnormalities (1,2). Autoantibodies and lymphopenia are often detected in SSc patients (2). $CD8^+$ T cells and $CD4^+$ Tregs have been shown to produce increased levels of the profibrotic cytokine IL-13 (3, 4), while NK cells have been reported to be less cytotoxic and have defects in IFN-γ production (5). However, while differences in cytokines produced in SSc may contribute to disease pathophysiology (6), the mechanisms underlying these changes in immune cell cytokine production remain largely unknown.

The function of T cells and NK cells is regulated by co-inhibitory receptors (co-IRs) such as PD-1, LAG-3, TIGIT, and TIM-3 (7,8). Engagement of these receptors by their ligands limits cytokine production in response to TCR or activating NK receptor stimulation. Co-IRs hence play critical physiological roles in limiting tissue damage from excessive immune activation. However, chronically increased expression of multiple co-IRs is a hallmark of immune exhaustion (9), where immune cells are no longer able to execute effector functions to fight chronic viral infections and cancer (10,11). In autoimmunity, co-IRs are protective: antibody blockade or genetic deletion of PD-1, TIM-3, TIGIT and LAG-3 in mouse models of autoimmune diseases such as type 1 diabetes, lupus and multiple sclerosis all result in accelerated or exacerbated disease (7). Treatment of cancer patients with co-IR blockade often precipitates autoimmune adverse events (12). As a corollary, reinforcing immune checkpoints in autoimmune disease may have therapeutic benefit. In support of this, an exhaustion-like phenotype marked by an increase in co-IR expression correlated with less flares in lupus patients (10), while the presence of $TIM\text{-}3^+$ T cells was associated with milder forms of multiple sclerosis (13). In SSc, a recent report indicates that the PD-1 pathway is involved in regulating disease severity (14).

Here, we determined the expression of the co-IRs, PD-1, TIGIT, TIM-3 and LAG-3 on lymphocyte subsets from peripheral blood of SSc patients, and assessed their role in cytokine regulation and fibroblast activation. PD-1, TIM-3 and TIGIT showed increased expression in specific T and NK cell subsets from SSc patients. Cytokine production in the presence of PD-1-, TIM-3- and TIGIT-blocking antibodies revealed significant patient-specific variation in function of individual co-IRs. In most subjects however, at least one co-IR was actively suppressing cytokine production, indicating the presence of exhausted cell populations. Multivariate analysis revealed that TIGIT and TIM-3 were functionally distinct from PD-1 in SSc patients, but not in healthy controls. Finally, changes in cytokines produced by PBMCs after TIM-3 blockade resulted in altered fibroblast gene expression.

Our study thus suggests that increased co-IR expression in SSc lymphocyte subsets contributes to patient-specific activities in modulating cytokine production. Suppressed and/or excessive production of specific cytokines in the local microenvironment may subsequently promote pathogenic fibrotic or inflammatory responses in connective tissue and vascular cells.

METHODS

Patients and controls

All samples and clinical data were collected under a protocol approved by the Institutional Review Board at Boston University. Blood samples were obtained from 30 SSc patients and 21 healthy patients in EDTA Blood Collection Tubes (BD Vacutainer®). Classification of patients was made according to ACR criteria (1). The patients had not received immunosuppressive therapy for at least six months prior to the blood draw. Patients and healthy controls were age matched.

Sample Collection

Blood samples were collected and PBMCs isolated the same day by under-laying Lymphoprep™ (Stem Cell) under blood and separating PBMCs by density dependent centrifugation. PBMC samples were frozen in 50% RPMI media (10% FBS, 1% non-essential amino acids, 1% HEPES, 1% PenStrep, 1% sodium pyruvate, 0.1% beta-mercaptoethanol) with 40% FBS and 10% DMSO and stored in liquid nitrogen.

Flow cytometric Analysis

PBMCs were thawed and stained as previously reported (15) on a BD FACSCARIA SORP with FACSDIVA software (BD Biosciences). Expert-guided gating was performed in FlowJo 10 and Cytobank by three independent analysts. T-SNE dimensionality reduction was performed using Cytobank platform with the following parameters: input of 500,000 single, live, CD14−/CD19− events; clustering channels (all arcsin-transformed): CD3, CD4, CD8, CD25, CD127, CD45RO, γδTCR, CD16, CD56, Vα24, CD1d-PBS57; total number of iterations: 3000; theta 0.5; perplexity 30.

In vitro Stimulation of PBMCs with allogeneic monocyte-derived dendritic cells

Monocyte derived dendritic cells (DCs) were produced after selection of CD14+ cells (Stem Cell Technologies) from PBMCs isolated from a Buffy Coat, using the manufacturer's instructions. CD14+ monocytes were cultured for 5 days in 7.5 ng/ml IL-4 (BD) and 20 ng/mL GMC-SF (Miltenyi Biotec). On day 4, 1 ng/ml of E. coli LPS (Sigma) was added to the cultures to mature the dendritic cells. Previously frozen PBMCs from patients and healthy controls were thawed and co-cultured with allogeneic DCs at 1:10 DCs to PBMCs with 5 μg/ml of blocking antibodies: anti-PD-1 (Clone J116, eBioScience), anti-TIGIT (Clone MBSA43, eBioScience), anti-TIM-3 (Clone F38-2E2, BioLegend), or Isotype control (Clone P3.6.2.8.1, eBioScience) in the presence of human Fc Block (BD). Cultures were kept at 37°C and 5% CO_2 for five days and supernatants were collected and stored at −80°C.

Multiplex Cytokine Analysis

Supernatants from in vitro stimulation cultures were analyzed using a 14-plex cytokine bead array kit (MILLIPLEX™ MAP Millipore Corporation, USA) on the Luminex 100 platform to determine cytokine concentrations. A human Th17 Magnetic Bead Panel (MILLIPLEX™ MAP HTH17MAG-14K-14) was used to detect concentrations of IFN-γ, IL-10, IL-13, IL-22, IL-9, IL-33, IL-2, IL-21, IL-4, IL-23, IL-5, IL-6, IL-27, and TNF-α. Data was analyzed using Milliplex Analysis 5.1 software. The standard curve was determined by interpolation from corresponding standards. IL-22 and IL-33 were excluded from analysis due to being below the limit of detection. Undetectable values were given an arbitrary value of 0. Values were clustered using Gene Cluster 3.0 and normalized, mean centered, and clustered by complete linage followed by visualization in JavaTree.

Fibroblast Cell Culture

SSc human dermal fibroblasts were grown to 80% confluence in DMEM with 10% FBS. 2.5×10^5 cells were serum-starved with media with 0.5% FBS overnight. Next, media was replaced with 50% supernatant from in vitro stimulated PBMC cultures and 50% RPMI with 10% FBS. Additional control cultures were set up with 10 ng/ml TGFβ1 (R&D), 30 ng/ml IL-13 (R&D), or no cytokines. Cells were incubated for 24 hours at 37°C, washed with PBS and lysed with RLT (Qiagen). RNA was collected with an RNeasy® Mini Kit (Qiagen).

Nanostring

100 ng of RNA was added to NanoString polymerase chain reaction tubes. 20 μl of Reporter CodeSet diluted in Buffer CodeSet and 5μl of Capture ProbeSet reagent (NanoString Technologies) was added to RNA. Sample was placed in MJ Mini thermocycler (BioRad) at 67°C. Samples were processed in an nCounter Prep Station (NanoString Technologies). Genes were normalized to a list of housekeeping genes, following a method previously described (16). Values were clustered using Gene Cluster 3.0 and normalized, mean centered, and clustered by complete linage followed by visualization in JavaTree.

Mathematical modeling

Partial least squares discriminant analysis (PLSDA) was conducted in MATLAB using the PLS Toolbox (Eigenvector Research, Inc.). Data was normalized along each parameter by Z-score before application of the algorithm. Cytokines or genes with non-zero values in fewer than half of subjects were excluded from analysis. Cross-validation was performed with one-fifth of the relevant dataset, and the number of latent variables (LVs) was chosen to minimize cross-validation error. Model confidence was calculated by randomly permuting the response variables 100 times and rebuilding the model to form a distribution of error for random models, and comparing our model to this distribution with the Mann-Whitney U test. Importance of each parameter to the model prediction was quantified using variable importance in projection (VIP) score. A VIP score greater than 1 (above average contribution) was considered important for model performance and prediction. The LASSO method was applied for variable selection in the gene expression data to determine the minimum gene set necessary for distinguishing treatment groups (Matlab, Mathworks). K-

fold cross-validation was utilized to optimize the set of gene parameters such that the error of the resulting model was minimized.

Statistical analysis

T tests were performed using the R function t.test with correction for multiple comparisons made with the R function p.adjust using the fdr parameter for false discovery rate.

RESULTS

Immunophenotyping of SSc PBMCs reveals increased co-IR expression in T and NK cell subsets

While the expression of co-IRs, as a hallmark of T cell exhaustion, has been associated with disease outcome in several autoimmune diseases, including lupus and type 1 diabetes (10), an extensive comparison of the expression of multiple co-IRs in SSc versus healthy subjects has not been performed. Therefore, we isolated PBMCs from SSc and age-matched healthy controls (Table 1) and stained the cells with a 16-color flow cytometry antibody panel to characterize expression of four co-IRs on various immune cell subsets simultaneously (15). Importantly, only patients that were not on immuno-suppressants were selected for our study, to rule out any role of immune-modulating drugs on expression levels. Twelve distinct immune cell types could be identified using an automated viSNE algorithm to blindly cluster cell subsets using fluorescence data (Fig. 1A). Expression of the co-IRs PD-1, TIM-3, TIGIT and LAG-3 showed significant cell-type specificity with PD-1 mostly expressed in $CD45RO^+$ memory T cells, TIGIT in T cells and NK cells and TIM-3 predominantly in NK cells (Fig. 1B). LAG-3 showed an overall low expression. To compare co-IR expression on blood lymphocyte subsets from SSc patients and healthy controls we defined ten distinct subsets of T and NK cells using a manual gating strategy (Supplemental Fig. 1). After exclusion of dead cells as well as $CD19^+$ B cells and $CD14^+$ monocytes, $CD3^+$ T cells were further divided in $CD4^+CD8^-$ T helper cells, $CD4^-CD8^+$ cytotoxic T cells, γδ T cells, and iNKT cells. Within the $CD4^+$ T cells, high expression levels of CD25 and low levels of CD127 were used to delineate a population enriched in regulatory T cells, hereafter referred to as “Tregs” (17,18). Since the $CD25^+CD127^{lo}$ phenotype does not 100% equate $Foxp3^+$ Tregs, it is critical to consider that changes in co-IR expression within this population may also represent a small subset of activated effector $CD4^+$ T cells. $CD4^+$ and $CD8^+$ T cell subsets were subdivided into $CD45RO^+$ memory and $CD45RO^-$ naive subsets (19) (Supplementary Fig. 1C). It is important to note here that we did not observe any differences in the frequencies of the major T cell types between the SSc and healthy control groups (Supplementary Fig. 2A), except for an increase in $CD25^+CD127^-$ Tregs in the SSc group (Supplemental Fig. 2B). Interestingly, the Treg subset showed a reduction of cells with a $CD45RO^+$ effector/memory phenotype in SSc patients (Supplementary Fig. 2C).

For $CD4^+$ Tconv cells, $CD4^+$ Tregs, and CD8+ T cells, PD-1, TIGIT, TIM-3 and LAG-3 expression was determined within the $CD45RO^+$ effector/memory population, since naïve T cells typically express low levels of these receptors; representative dot plots of co-IR staining are shown in Supplementary Fig. 3. In SSc patients, the numbers of PD-1-expressing cells within the Treg subset and within γδ T cells were significantly increased,

compared to healthy subjects, while no changes in PD-1 expression were observed on $CD8^+$ T cells, iNKT cells, or NK cell subsets (Fig. 1C). The difference in PD-1 expression on $CD4^+$ Tconv cells did not reach statistical significance after a false discovery rate analysis, but strongly trended towards and increase ($p = 0.054$) (Fig. 1C). TIGIT was enhanced on $CD4^+$ Tconv, Tregs and $CD8^+$ T cells from SSc patients, but not γδ T cells, iNKT cells, and NK cells thus showing a somewhat different pattern than PD-1 (Fig. 1D). TIM-3 showed low expression levels on all T cell subsets, confirming viSNE analysis, and no changes between healthy controls and SSc patients (Fig. 1E). As noted above, TIM-3 was strongly present on NK cells and further increased on the $CD16^+CD56^{med}$ subset in SSc patients. LAG-3 was minimally present on all analyzed subsets and there were no noteworthy changes between healthy subjects and SSc patients (Fig. 1F). Not surprisingly, co-IRs were less expressed in $CD45RO^-$ naive Tconv, Tregs, and $CD8^+$ cells although some differences in SSc patients were still apparent (Supplementary Fig. 4).

Finally, we performed a separate analysis of patients with high percentages of Tregs (Supplementary Fig. 5). We determined that the presence of significantly more Tregs (or $CD25^+CD127^{lo}$ activated effector cells) in seven patients could not be attributed to SSc disease type (limited versus diffuse) or the presence or absence of lung and skin involvement (data not shown). Intriguingly, patients with high Treg percentages also had increased co-IR expression (Supplementary Fig. 5), potentially suggestive of a more “activated” disease environment in these patients, leading to Treg expansion and enhanced co-IR expression.

SSc patients show an increased frequency of T lymphocytes co-expressing PD-1 and TIGIT

One hallmark of exhausted T cells is the accumulated expression of multiple co-IRs on the cell surface (9). Comprehensive co-IR signature analysis revealed that $CD4^+$ Tconv cells and Tregs from SSc patients contained an increased frequency of $PD\text{-}1^+$ $TIGIT^+$ double positive cells, compared to healthy subjects (Fig. 2). In NK $CD56^{med}$ cells, co-expression of TIGIT and TIM-3 showed a trend towards increased presence in SSc patients vs healthy controls (data not shown). The increased presence of T cells expressing combinations of co-IRs in SSc patients suggested an increased level of immune dysfunction and exhaustion in those patients. Perhaps surprisingly, this increased exhaustion signature, as well as the increases in single co-IR-positive populations described above, did not correlate with disease duration (data not shown). The striking exhaustion phenotype however prompted us to investigate the functional role of co-IRs in the activation of T cells from SSc patients.

PD-1, TIGIT and TIM-3 exhibit patient-specific activity in controlling T cell cytokine production

To directly test whether co-IRs differentially regulate T cell responses in SSc patients and healthy subjects, we designed an assay using monocyte-derived DCs from a healthy donor as an allogeneic stimulus in a mixed lymphocyte reaction (MLR). This assay requires cognate T cell -DC interactions for T cell activation and hence facilitates physiologic engagement of co-IRs on the T cells with their ligands on the DCs (20). For this reason an MLR is often used to test the functionality of novel checkpoint inhibitors for cancer immunotherapy (21–23). By using the same DC donor to stimulate responders, differing amounts of inhibitory

receptor ligands present on DCs were eliminated as a variable. Blocking antibodies for PD-1, TIGIT, and TIM-3 were added to the MLR to prevent the binding of ligands to the receptors. In a first set of experiments, we confirmed that antibody treatment did not affect the viability or ratios of the $CD4^+$ and $CD8^+$ T cell subsets in the MLR cultures (Supplementary Fig. 6). Next, supernatants from MLR cultures were collected and the presence of fourteen cytokines measured using a multiplex platform. As expected, the amount and types of cytokines produced by individual subjects showed significant variability (Fig. 3). Nevertheless, two distinct profiles could be readily observed: subjects showing a response dominated by the pro-inflammatory cytokines IFN-γ, IL-6 and TNFα (HC#1, #2, #3 and #4; SSc#1, SSc#2, SSc#3) vs subjects with a more diverse cytokine response and increased presence of Th2 cytokines (HC#5, SSC#4, SSc#5, SSc#6). In most cases, co-IR blockade did not appear to selectively promote the production of specific cytokines and hence did not lead to dramatic changes in the composition of patient-specific cytokine profiles (Fig. 3). In 4/5 healthy and 4/6 SSc individuals, at least two of the co-IR-blocking antibodies increased the total amount of cytokines produced. In both healthy and SSc subjects, PD-1 appeared the strongest regulator of cytokine secretion (Fig. 3, Fig. 4A). However, in SSc patients, the role of TIGIT and TIM-3 was modest, while in most healthy subjects TIGIT and/or TIM-3 were potent secondary regulators of total cytokine secretion (Fig. 4A). Interestingly, there was significant patient-specific variation in cytokine-regulating activities of co-IRs. This experiment demonstrated that co-IR expression in SSc PBMCs is not exclusively a marker of a dysfunctional immune system, but that interactions of co-IRs with their ligands can actively regulate T cell effector functions and hence may play a role in T cell-dependent pathogenic processes in SSc.

To establish whether co-IR blockade during MLR cultures affected the cytokine response of healthy and SSc immune cells differentially, the large data set was analyzed using advanced bioinformatics and mathematical modeling. Unsupervised hierarchical clustering of cultures from subjects with various treatments and cytokines resulted in donors, rather than treatment groups, clustering together, masking any indication of potential effects of the blocking antibodies on cytokine production (Supplementary Fig. 7A). Therefore, to determine whether the activities of PD-1, TIGIT and TIM-3 in SSc and healthy subjects could be differentiated, we performed Partial Least Squared Regression Discriminant Analysis (PLSDA). PLSDA is a mathematical analysis method that uses latent variables (LVs) to determine which parameters contribute to causing the greatest difference between samples. PLSDA is useful when the behavior of multiple analytes of interest, in this case cytokines, are known to be interdependent and can reveal combinations of cytokines whose fluctuation as a group maximally correlates with the anti-co-IR antibody treatments (24,25). Samples of each treatment group were normalized relative to isotype-treated controls to account for the large differences in total cytokine produced between subjects. Then, samples were mapped onto three dimensional latent variable space and connected with lines that meet at their centroid (Figure 4B). In SSc subjects our analysis showed that cytokine secretion profiles differed in anti-PD-1-treated cells, compared to anti-TIM-3 and -TIGIT, with a model confidence of 88%; this distinction was not found in samples from healthy controls (Figure 4C). The PLSDA model was unable to show any differences between anti-TIGIT or anti-TIM-3 in healthy controls and SSc subjects. Multiple cytokines contributed to LV1, which

separated anti-PD-1 treatment from anti-TIGIT and -TIM-3 in SSc patients (Fig. 4D). Increased overall production of IL-10, IL-13, IL-2, IL-21, and IL-4 in the anti-PD-1 treated SSc samples most significantly contributed to the distinction, as determined by VIP score. This analysis thus strengthens the conclusion that in SSc patients PD-1 continued to exert its normal function of actively inhibiting T cell cytokine production, but the TIGIT and TIM-3 pathways, while actively controlling cytokine secretion in healthy controls, became defective or refractory to reversal. Such a separation between the functionality of PD-1 on the one hand and TIGIT/TIM-3 on the other hand, has not been previously demonstrated in a human autoimmune disease.

Altered T cell cytokine production after co-IR blockade modulates SSc fibroblast activation

Much of the pathogenesis of SSc is driven by fibrosis in target organs. It is thought that pathogenic fibroblasts produce large amounts of collagen leading to loss of cellularity and elasticity in the skin and internal organs (26). To explore whether blocking co-IRs on T cells could have a potential effect on this cell type, we cultured SSc primary fibroblasts for 24 hours with the supernatants collected from MLR cultures in Fig. 3. Fibroblasts were washed and RNA isolated for NanoString analysis of genes previously described to be important for SSc disease pathogenesis (16). Interestingly, hierarchical clustering revealed that the two main clusters are largely driven by the two distinct cytokine signatures identified in Fig. 3: the “pro-inflammatory” group and the “diverse/Th2” group (Supplementary Fig. 7B). Within these two groups, donor-specific patterns of gene expression appeared the most similar. Since our data in Fig. 3 demonstrated that blocking co-IRs mostly resulted in quantitative, rather than qualitative, changes in cytokine production, it is perhaps not surprising that supernatants from treated cultures did not cause uniformly clustered changes in the basic fibroblast gene expression patterns. Next, we examined whether multivariate mathematical modeling was capable of distinguishing the effects of anti-co-IR treatment on fibroblast gene expression after exposure to culture supernatants. Feature selection using the LASSO algorithm was performed, resulting in narrowing our gene set from 53 to 21 genes. Subsequently, PLSDA was applied to identify patterns of gene expression that differentiated the treatment groups. Surprisingly, we found that fibroblasts treated with supernatants from anti-TIM-3-treated MLRs from both SSc patients and healthy controls had a distinctly modified gene expression profile from the anti-PD-1 and anti-TIGIT treatments (Figure 5A). This distinct gene expression profile from the anti-TIM-3 group separated based on LV1 (Figure 5B). Since TIM-3 did not strongly regulate the 12 measured cytokines in SSc lymphocytes (Fig. 3, 4A, B), it is likely that an unknown factor, induced after TIM-3 blockade, is an important regulator of SSc fibroblast gene expression. Importantly, the main drivers of LV1 were pro-fibrotic genes, suggesting that TIM-3 might play a protective role in SSc fibrosis. Contrary to TIM-3, anti-PD-1 treatment did not appear to drive gene expression changes in fibroblasts, suggesting that PD-1 mostly controls the amount of cytokines produced, without significantly changing the composition of the supernatants.

DISCUSSION

In this study we analyzed the expression and function of the co-IRs PD-1, TIM-3, TIGIT and LAG-3 in SSc PBMCs. PD-1 and TIGIT are increased and co-expressed on multiple T

cell subsets from SSc patients while TIM-3 is increased on the cytotoxic $CD16^{+}CD56^{med}$ subset of NK cells. Co-IRs play distinct roles in regulating the production of cytokines and their functionality differed significantly between individual donors. Importantly, TIGIT and TIM-3, but not PD-1, showed reduced activity in SSc patients vs. healthy controls. Our observations thus support a cell-specific altered expression pattern of co-IRs in SSc immune cells, rather than a broad upregulation of these receptors. Moreover, co-IRs play complex and patient-specific roles in regulating cytokine production, a finding with potential implications for better understanding this heterogeneous disease.

SSc is a poorly understood autoimmune disorder that produces extreme reduction in quality of life and currently has a ten year fifty percent survival rate (27). Patients have few treatment options and a greater understanding of the underlying immunological mechanisms of the disease is needed to assess the feasibility of developing immunotherapies. While many studies have focused on understanding aberrant fibroblast differentiation in SSc, there is also evidence that immune cells and the cytokines they produce play a critical role in fibrosis. In many fibrotic diseases, it is well-established that Th2 type immune responses, producing IL-4 and IL-13, promote fibrosis (28). T-cell-derived TGF-β may contribute as well (29). In SSc however, robust evidence for a critical role of bona fide Th2 cells remains limited (30). $CD8^{+}$ T cells may also be a source of IL-13, as was demonstrated by Fuschiotti *et al.* in SSc peripheral blood (4) and skin (31). One intriguing study demonstrated that skin Tregs can produce IL-4 and IL-13, possibly contributing to a fibrotic phenotype (5). This finding, combined with studies indicating that bona fide $Foxp3^{+}$ Tregs numbers are reduced in the skin of SSc patients (32,33) suggests Treg deficiencies play a role in SSc. It would be of interest to determine whether our observation that $CD45RO^{+}$ effector/memory Tregs are specifically reduced in SSc blood correlates with the reported decrease in tissue-resident Tregs. A number of recent studies indicate that Th17 cells are present in SSc and may contribute to the disease process (34,35). Together, these studies underscore the need for a better understanding of the regulatory mechanisms underlying the potential pro-fibrotic and pro-inflammatory functions of various T cell subsets in SSc.

Co-IRs such as PD-1, TIM-3, LAG-3 and TIGIT are an important class of molecules controlling T cell effector responses. Our finding that these receptors are aberrantly expressed in SSc patients is in line with the general trend for these receptors to be increased in other rheumatic diseases. However, the co-IR expression patterns on various lymphocyte subsets show considerable disease-dependent variation. For example, PD-1 is increased in $CD4^{+}$ and $CD8^{+}$ T and NK cells from lupus patients (36,37), and in $CD3^{+}$ T cells from psoriatic arthritis patients (38), while in SSc it is only significantly enhanced in Tregs and γδ T cells (Fig. 1C). In addition, serum levels of soluble forms of PD-1 and its ligand PD-L2 were recently shown to be elevated in SSc (14). Li et al. describe increased TIM-3 on $CD4^{+}$ and $CD8^{+}$ T cells in peripheral blood from rheumatoid arthritis patients (39), while our data show no changes in TIM-3 in SSc T cell subsets, but an increase in NK cells (Fig. 1E). In lupus, TIGIT is upregulated on $CD4^{+}$ T cells but reduced in $CD8^{+}$ T cells, NK cells and Tregs (40), an expression pattern that also does not match with SSc (Fig. 1D). Deciphering the origin and functional consequences of these differences constitutes an important future research direction.

Co-IRs have been demonstrated to play critical functional roles in in vivo models of autoimmune disorders (7) and in chronic viral infections and cancer (9). In HIV and cancer increased expression of PD-1 and the co-expression of multiple co-IRs is linked with a corresponding decrease in effector function of T cells (9), a state described as “T cell exhaustion”. Blocking co-IRs can restore effector function, as has been shown in successful immunotherapy for cancer (41,42). However, epigenetic mechanisms dictating exhaustion can provide a barrier to lymphocyte rejuvenation (43). Our findings that anti-TIGIT and anti-TIM-3 were largely ineffective in enhancing cytokine production in PBMCs from SSc patients, and that SSc patients showed increased numbers of PD-1^+ $TIGIT^+$ double positive T cells, suggest that a more robust state of T cell exhaustion, perhaps epigenetically controlled, is present in SSc patients compared to healthy controls. Our antibody blocking experiments revealed that PD-1 played the most dominant role in modulating cytokine secretion. PD-1 has extensively been characterized as limiting the production of cytokines in immune cells. It is therefore feasible that increased PD-1 expression in SSc represents a regulatory mechanism attempting to limit tissue damage. However, absence of the ligands engaging PD-1 in the tissue microenvironment may preclude successful engagement of this pathway. Alternatively, PD-1, TIM-3 and TIGIT may suppress some T cell cytokines but not others, leading to subtle skewing of cytokine profiles. Such changes in cytokine signatures due to aberrant expression of co-IR combinations and, perhaps, their ligands in fibrotic tissues may impinge on disease processes. In support of this hypothesis, our data show that co-IR blockade during an in vitro immune response provokes changes in soluble factors that can have an impact on fibroblast gene expression. In some cases, these changes may be caused by the cytokines we measured and that have known activities in fibroblasts. IL-13 for example is a potent inducer of collagen production (44). One intriguing possibility however, revealed by mathematical modeling, was that TIM-3 modulated the production of unidentified soluble factors that had a distinct effect on SSc fibroblast gene expression. One obvious candidate to initiate these changes would be the pro-fibrotic cytokine TGF-β, but recombinant TGF-β alone was not able to recapitulate the gene expression profile induced by any of the co-IR blocking antibodies (data not shown).

In summary, our study documents that SSc patients express co-IR signatures reminiscent of immune cell exhaustion. Functional analysis and mathematical modeling of the impact of these co-IRs on disease-relevant cytokine production and fibroblast gene expression, suggests that these pathways play a role in SSc pathophysiology and may be amenable targets for therapy.

Supplementary Material

Refer to Web version on PubMed Central for supplementary material.

Acknowledgments

The authors thank Nina Kishore and Eric Stratton for help with patient enrollment, and Ashna Gupta for assistance with clinical data analysis. Technical support was provided by the Boston University Analytical Core (Matthew Au) and Flow Cytometry Core Facility. The authors thank the patients for their participation in the study. The work in this manuscript was supported by start-up funds from the BU Department of Medicine, Rheumatology Section (H.D.), National Institutes of Arthritis, Musculoskeletal and Skin Disease grant 1P50AR060780 “Scleroderma

Center of Research Translation" (R.L.), and National Institute of Allergy and Infectious Diseases grant T32AI007309 "Research Training in Immunology" (M.F.).

References

1. Van Den Hoogen F, Khanna D, Fransen J, Johnson SR, Baron M, Tyndall A, et al. 2013 classification criteria for systemic sclerosis: An american college of rheumatology/European league against rheumatism collaborative initiative. Arthritis Rheum. 2013; 65:2737–2747. [PubMed: 24122180]
2. Allanore Y, Simms R, Distler O, Trojanowska M, Pope J, Denton CP, et al. Systemic sclerosis. Nat Rev Dis Prim. 2015:15002. [PubMed: 27189141]
3. Almeida I, Silva SV, Fonseca AR, Silva I, Vasconcelos C, Lima M. T and NK Cell Phenotypic Abnormalities in Systemic Sclerosis: a Cohort Study and a Comprehensive Literature Review. Clin Rev Allergy Immunol. 2015; 49:347–369. [PubMed: 26445774]
4. Fuschiotti P, Medsger TA, Morel PA. Effector CD8+ T cells in systemic sclerosis patients produce abnormally high levels of interleukin-13 associated with increased skin fibrosis. Arthritis Rheum. 2009; 60:1119–1128. [PubMed: 19333920]
5. Macdonald KG, Dawson NAJ, Huang Q, Dunne JV, Levings MK, Broady R. Regulatory T cells produce profibrotic cytokines in the skin of patients with systemic sclerosis. J Allergy Clin Immunol. 2015; 135:946–955. e9. [PubMed: 25678090]
6. Baraut J, Michel L, Verrecchia F, Farge D. Relationship between cytokine profiles and clinical outcomes in patients with systemic sclerosis. Autoimmun Rev. 2010; 10:65–73. [PubMed: 20713187]
7. Anderson AC, Joller N, Kuchroo VK. Lag-3, Tim-3, and TIGIT: Co-inhibitory Receptors with Specialized Functions in Immune Regulation. Immunity. 2016; 44:989–1004. [PubMed: 27192565]
8. Ferris RL, Lu B, Kane LP. Too Much of a Good Thing? Tim-3 and TCR Signaling in T Cell Exhaustion. J Immunol. 2014; 193:1525–1530. [PubMed: 25086175]
9. Wherry EJ. T cell exhaustion. Nat Immunol. 2011; 12:492–499. [PubMed: 21739672]
10. McKinney EF, Lee JC, Jayne DR, Lyons PA, Smith KG. T-cell exhaustion, co-stimulation and clinical outcome in autoimmunity and infection. Nature. 2015; 523:612–616. [PubMed: 26123020]
11. Day CL, Kaufmann DE, Kiepiela P, Brown Ja, Moodley ES, Reddy S, et al. PD-1 expression on HIV-specific T cells is associated with T-cell exhaustion and disease progression. Nature. 2006; 443:350–4. [PubMed: 16921384]
12. June CH, Warshauer JT, Bluestone JA. Is autoimmunity the Achilles' heel of cancer immunotherapy? Nat Med. 2017; 23:540–547. [PubMed: 28475571]
13. Saresella M, Piancone F, Marventano I, Rosa F, La Tortorella P, Caputo D, et al. A role for the TIM-3/GAL-9/BAT3 pathway in determining the clinical phenotype of multiple sclerosis. FASEB J. 2014; 28:5000–5009. [PubMed: 25091272]
14. Fukasawa T, Yoshizaki A, Ebata S, Nakamura K, Saigusa R, Miura S, et al. Soluble form of PD-1 and PD-L2 contributes to disease severity and progression in systemic sclerosis. Arthritis Rheumatol. 2017; 11:300–308.
15. Belkina AC, Snyder-Cappione JE. OMIP-037: 16-color panel to measure inhibitory receptor signatures from multiple human immune cell subsets. Cytom Part A. 2017; 91:175–179.
16. Rice LM, Ziemek J, Stratton EA, McLaughlin SR, Padilla CM, Mathes AL, et al. A Longitudinal Biomarker for the Extent of Skin Disease in Patients With Diffuse Cutaneous Systemic Sclerosis. Arthritis Rheumatol. 2015; 67:3004–3015. [PubMed: 26240058]
17. Liu W, Putnam AL, Xu-yu Z, Szot GL, Lee MR, Zhu S, et al. CD127 expression inversely correlates with FoxP3 and suppressive function of human CD4 $^{+}$ T reg cells. J Exp Med. 2006; 203:1701–1711. [PubMed: 16818678]
18. Seddiki N, Santner-Nanan B, Martinson J, Zaunders J, Sasson S, Landay A, et al. Expression of interleukin (IL)-2 and IL-7 receptors discriminates between human regulatory and activated T cells. J Exp Med. 2006; 203:1693–1700. [PubMed: 16818676]

19. Rothstein DM, Yamada A, Farber D, Medical H. Cyclic regulation of CD45 isoform expression in a long term human CD4 + CD45RA + T cell. The Journal of Immunology. 1991; 146:1175–1183. [PubMed: 1671403]
20. Stecher C, Battin C, Leitner J, Zettl M, Grabmeier-Pfistershammer K, Höller C, et al. PD-1 blockade promotes emerging checkpoint inhibitors in enhancing T Cell responses to allogeneic dendritic cells. Front Immunol. 2017; 8:1–13. [PubMed: 28149297]
21. Wang C, Thudium KB, Han M, Wang X-T, Huang H, Feingersh D, et al. In Vitro Characterization of the Anti-PD-1 Antibody Nivolumab, BMS-936558, and In Vivo Toxicology in Non-Human Primates. Cancer Immunol Res. 2014; 2:846–856. [PubMed: 24872026]
22. Stewart R, Morrow M, Hammond SA, Mulgrew K, Marcus D, Poon E, et al. Identification and Characterization of MEDI4736, an Antagonistic Anti-PD-L1 Monoclonal Antibody. Cancer Immunol Res. 2015; 3:1052–1062. [PubMed: 25943534]
23. Lázár-Molnár E, Scandiuzzi L, Basu I, Quinn T, Sylvestre E, Palmieri E, et al. Structure-guided development of a high-affinity human Programmed Cell Death-1: Implications for tumor immunotherapy. EBioMedicine. 2017; 17:30–44. [PubMed: 28233730]
24. Lau KS, Cortez-Retamozo V, Philips SR, Pittet MJ, Lauffenburger DA, Haigis KM. Multi-Scale In Vivo Systems Analysis Reveals the Influence of Immune Cells on TNF-α-Induced Apoptosis in the Intestinal Epithelium. PLoS Biol. 2012:10.
25. Blanche, Ip, Cilfone, Nicholas, Belkina, Anna C., DeFuria, Jason, Jagannathan-Bogdan, Madhumita, Zhu, Min, Kuchibhatla, Ramya, McDonnell, Marie E., Xiao, Qiang, Kepler, Thomas B., Apovian DAL, Caroline M., Nikolajczyk, BS. Th17 cytokines differentiate obesity from obesity-associated type 2 diabetes and promote TNFα production Blanche. Obesity. 2016; 24:102–112. [PubMed: 26576827]
26. Pattanaik D, Brown M, Postlethwaite BC, Postlethwaite AE. Pathogenesis of systemic sclerosis. Front Immunol. 2015:6. [PubMed: 25688242]
27. Elhai M, Meune C, Avouac J, Kahan A, Allanore Y. Trends in mortality in patients with systemic sclerosis over 40 years: a systematic review and meta-analysis of cohort studies. Rheumatology. 2012; 51:1017–1026. [PubMed: 21900368]
28. Wynn TA. Type 2 cytokines: mechanisms and therapeutic strategies. Nat Rev Immunol. 2015; 15:271–282. [PubMed: 25882242]
29. Roberts AB, Sporn MB, Assoian RK, Smith JM, Roche NS, Wakefield LM, et al. Transforming growth factor type beta: rapid induction of fibrosis and angiogenesis in vivo and stimulation of collagen formation in vitro. Proc Natl Acad Sci. 1986; 83:4167–4171. [PubMed: 2424019]
30. O'Reilly S, Hügle T, van Laar JM. T cells in systemic sclerosis: a reappraisal. Rheumatology. 2012; 51:1540–9. [PubMed: 22577083]
31. Fuschiotti P, Larregina AT, Ho J, Feghali-Bostwick C, Medsger TA. Interleukin-13-producing CD8+ T cells mediate dermal fibrosis in patients with systemic sclerosis. Arthritis Rheum. 2013; 65:236–246. [PubMed: 23001877]
32. Antiga E, Quaglino P, Bellandi S, Volpi W, Bianco E, Del Comessatti A, et al. Regulatory T cells in the skin lesions and blood of patients with systemic sclerosis and morphoea. Br J Dermatol. 2010; 162:1056–1063. [PubMed: 20105169]
33. Klein S, Kretz CC, Ruland V, Stumpf C, Haust M, Hartschuh W, et al. Reduction of regulatory T cells in skin lesions but not in peripheral blood of patients with systemic scleroderma. Ann Rheum Dis. 2011; 70:1475–1481. [PubMed: 21097800]
34. Radstake TRDJ, Bon L, van Broen J, Hussiani A, Hesselstrand R, Wuttge DM, et al. The pronounced Th17 profile in systemic sclerosis (SSc) together with intracellular expression of TGFβ and IFNγ distinguishes SSc phenotypes. PLoS One. 2009:4.
35. Fenoglio D, Battaglia F, Parodi A, Stringara S, Negrini S, Panico N, et al. Alteration of Th17 and Treg cell subpopulations co-exist in patients affected with systemic sclerosis. Clin Immunol. 2011; 139:249–257. [PubMed: 21419712]
36. Bertsias GK, Nakou M, Choulaki C, Raptopoulou A, Papadimitraki E, Goulielmos G, et al. Genetic, immunologic, and immunohistochemical analysis of the programmed death 1/programmed death ligand 1 pathway in human systemic lupus erythematosus. Arthritis Rheum. 2009; 60:207–218. [PubMed: 19116915]

37. Jiao Q, Liu C, Yang Z, Ding Q, Wang M, Li M, et al. Upregulated PD-1 expression is associated with the development of systemic lupus erythematosus, but not the PD-1. 1 Allele of the PDCD1 gene. Int J Genomics. 2014; 2014:10–12.

38. Peled M, Strazza M, Azoulay-Alfaguter I, Mor A. Analysis of Programmed Death-1 in Patients with Psoriatic Arthritis. Inflammation. 2015; 38:1573–1579. [PubMed: 25663558]

39. Li S, Peng D, He Y, Zhang H, Sun H, Shan S, et al. Expression of TIM-3 on CD4+ and CD8+ T cells in the peripheral blood and synovial fluid of rheumatoid arthritis. APMIS. 2014:1–6.

40. Mao L, Hou H, Wu S, Zhou Y, Wang J, Yu J, et al. TIGIT signalling pathway negatively regulates $CD4^+$ T-cell responses in systemic lupus erythematosus. Immunology. 2017; 151:280–290. [PubMed: 28108989]

41. Topalian SL, Sznol M, McDermott DF, Kluger HM, Carvajal RD, Sharfman WH, et al. Survival, Durable Tumor Remission, and Long-Term Safety in Patients With Advanced Melanoma Receiving Nivolumab. J Clin Oncol. 2014; 32:1020–1030. [PubMed: 24590637]

42. Yang Y. Cancer immunotherapy: Harnessing the immune system to battle cancer. J Clin Invest. 2015; 125:3335–3337. [PubMed: 26325031]

43. Ghoneim HE, Fan Y, Moustaki A, Abdelsamed HA, Dash P, Dogra P, et al. De Novo Epigenetic Programs Inhibit PD-1 Blockade-Mediated T Cell Rejuvenation. Cell. 2017; 170:142–157. e19. [PubMed: 28648661]

44. Chiaramonte MG, Donaldson DD, Cheever AW, Wynn TA. An IL-13 inhibitor blocks the development of hepatic fibrosis during a T-helper type 2–dominated inflammatory response. J Clin Invest. 1999; 104:777–785. [PubMed: 10491413]

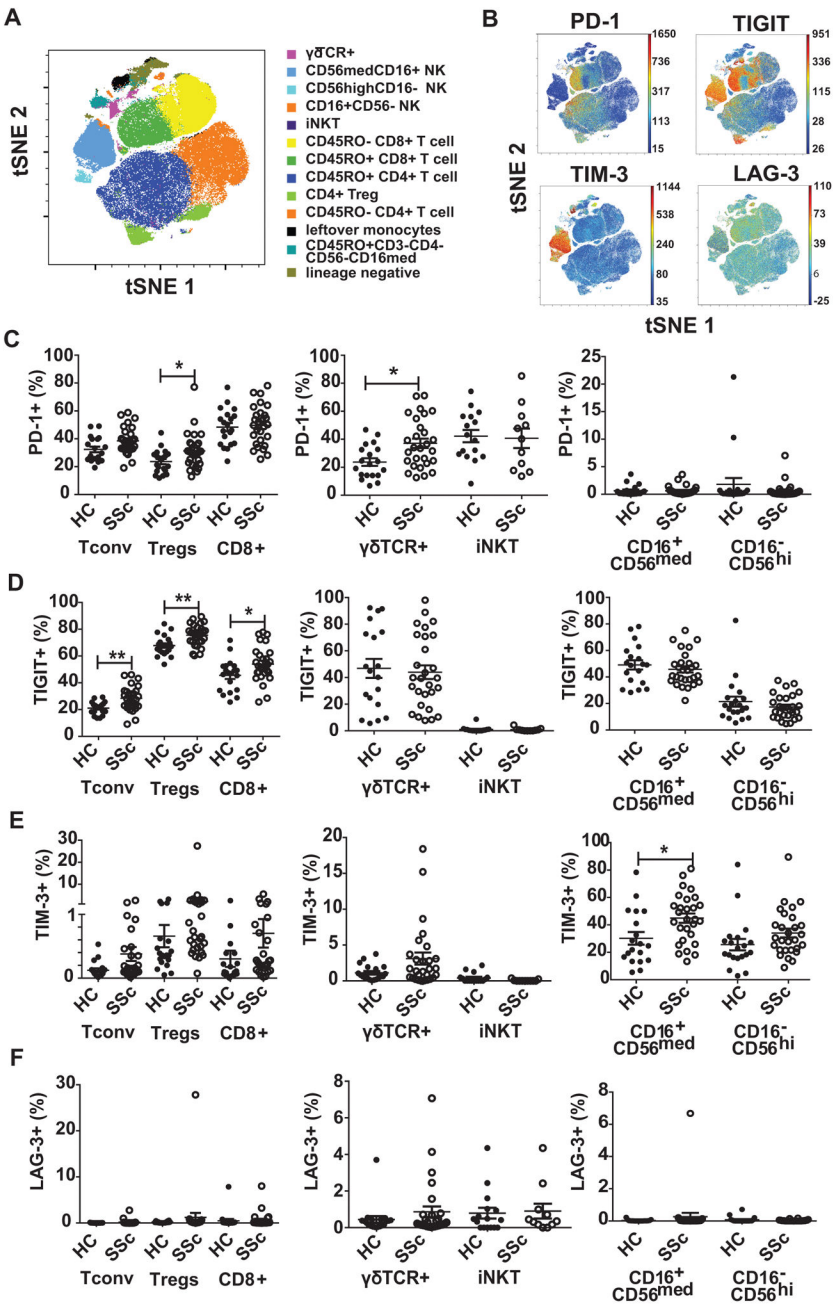

FIGURE 1. SSc patients express increased levels of PD-1, TIGIT and TIM-3 in defined peripheral blood lymphocyte subsets

PBMCs were isolated from SSc patients and healthy controls and the cells stained with a 16-color antibody panel for flow cytometric analysis. (A) Single live $CD19^{-}CD14^{-}$ events were gated from flow cytometry data of a representative subject and t-SNE dimension reduction was applied with lineage marker channels used for clustering. Populations were gated manually as in Supplementary Fig. 1 and events overlaid on the t-SNE map to show positioning of 12 separate subsets of immune cells. (B) t-SNE plots showing the expression of PD-1, TIGIT, TIM-3 and LAG-3 on immune cell subsets mapped as in A (color scale

depicts fluorescence intensity as a measure of expression level). (C–E) Using manual gating, the percentage of PD-1^+ (C), TIGIT$^+$ (D), TIM-3^+ (E) and LAG-3^+ (F) cells within $CD4^+CD25^{lo}CD45RO^+$ Tconv cells, $CD4^+CD25^{hi}CD127^{lo}CD45RO^+$ Tregs, $CD8^+CD45RO^+$ T cells, γδ TCR^+ T cells, iNK T cells, $CD16^+CD56^{med}$ NK cells and $CD16^-CD56^{hi}$ NK cells was determined. Each symbol represents an individual subject. Mean ± SEM is indicated. iNKT cells only shown if >20 events were recorded. Statistics was done with t test with false discovery rate adjustment * $p \leq 0.05$

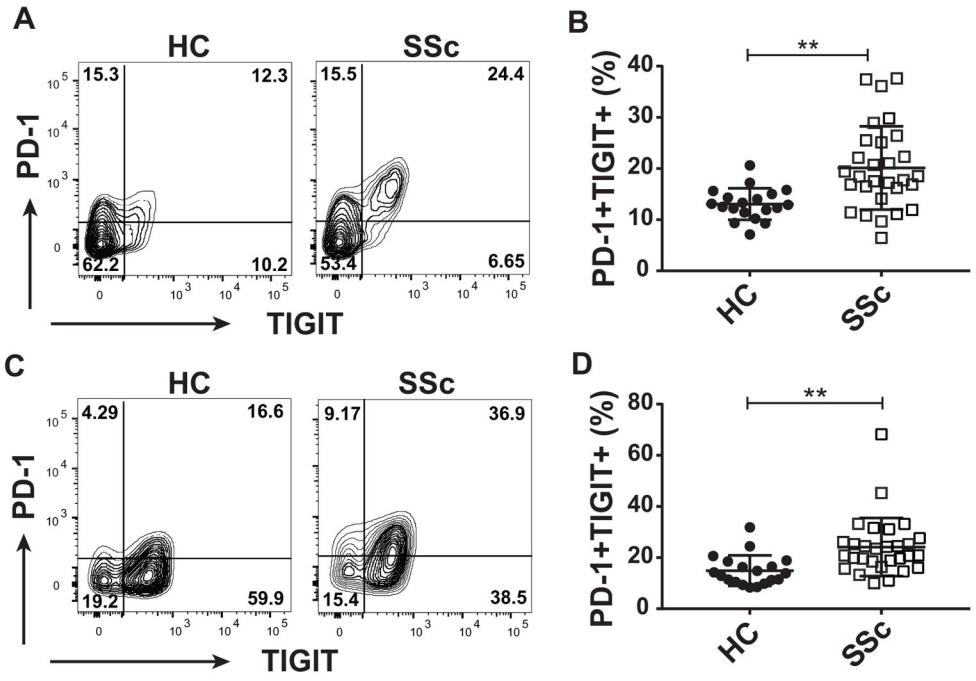

FIGURE 2. SSc patients contain increased levels of PD-1$^+$ TIGIT$^+$ double positive T cells

Co-expression of PD-1 and TIGIT on lymphocyte subsets form Fig. 1 was analyzed using manual gating. (A) Representative dot plots of PD-1$^+$ TIGIT$^+$ double positive cells in CD4$^+$ Tconv cells of healthy controls (HC) and SSc patients (B) Graph shows percentages of PD-1$^+$ TIGIT$^+$ Tconv cells from all subjects. (C) Representative dot plots of PD-1$^+$ TIGIT$^+$ double positive Tregs in HC and SSc patients. (D) Graph shows percentages of PD-1$^+$ TIGIT$^+$ Tregs from all subjects. ** p≤ 0.01

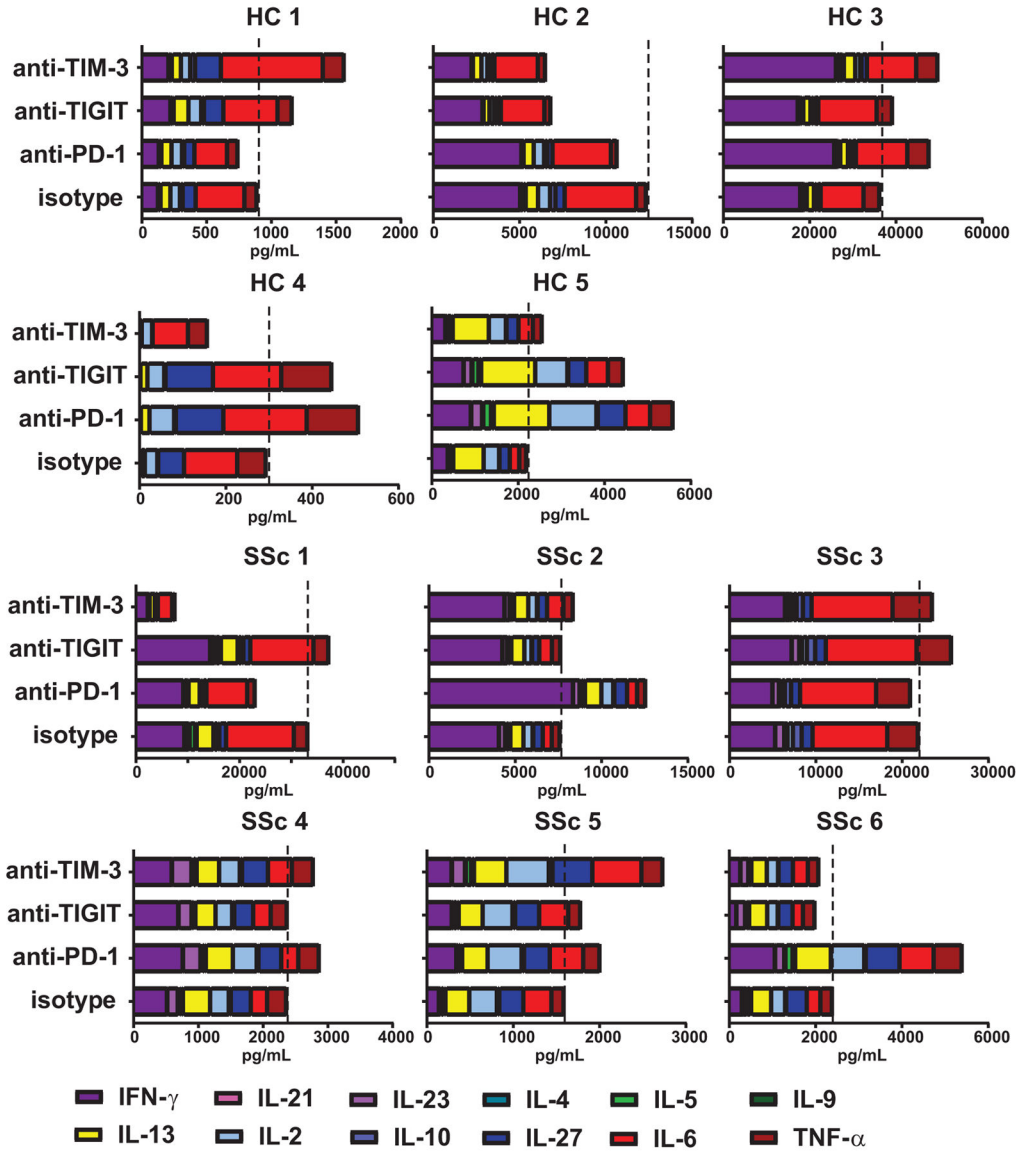

FIGURE 3. Co-IRs exhibit subject-specific activities in controlling lymphocyte cytokine production

PBMCs from SSc and healthy subjects were stimulated with DCs from a healthy donor in the absence or presence of anti-PD-1, anti-TIGIT or anti-TIM blocking antibodies and supernatants analyzed with a 14 cytokine multiplex assay. Bar graphs show the amount (pg/ml) of each of the indicated cytokines produced by individual healthy and SSc donors. Dotted line indicates the level of total cytokine produced in the isotype control cultures.

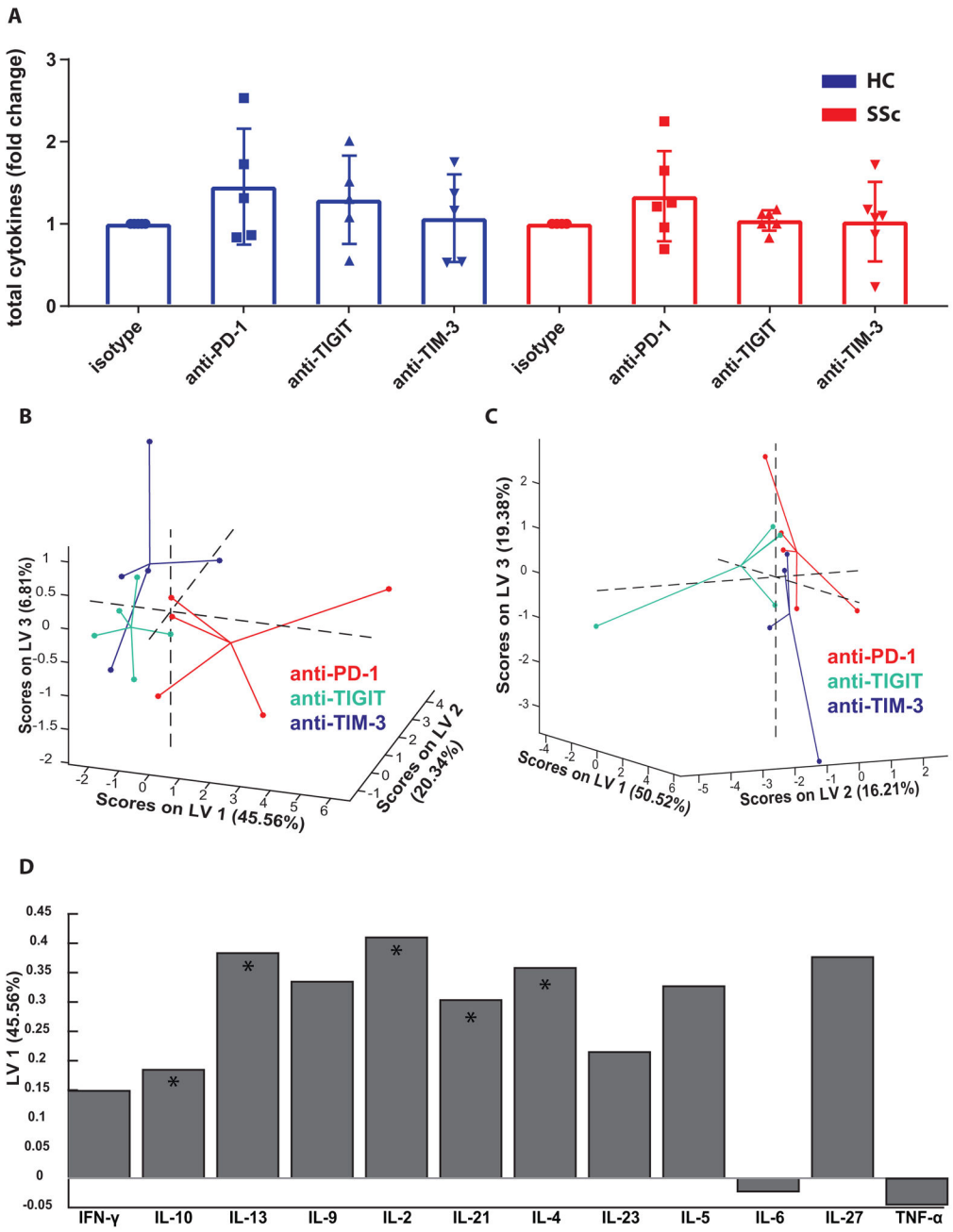

FIGURE 4. Blocking PD-1, but not TIGIT and TIM-3, modulates cytokine production in SSc PBMCs

(A) Graphs show the fold change of total measured cytokines after co-IR blockade relative to isotype controls, as calculated from the data in Fig. 3. Each symbol represents an individual donor. Bars show the average ± SEM. (B–D) Multiplex cytokine data was subjected to PLSDA to identify variations in patterns of cytokine production caused by co-IR blocking antibodies, after normalization with isotype control values. Graphs show data points from each culture condition of SSc (B) and healthy (C) donors mapped onto three dimensional LV space and connected with lines that meet at their centroid. (D) Bar graph

shows the contribution of cytokines from SSc MLR cultures to LV1. Asterisks designate cytokines that contributed most to LV1 separation in this model, as determined by VIP score.

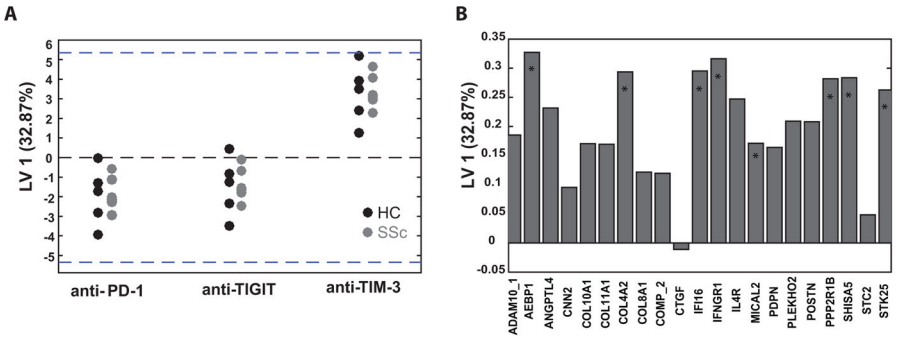

FIGURE 5. Blocking TIM-3 in MLR cultures promotes the production of soluble factors altering SSc fibroblast gene expression

SSc fibroblasts were cultured for 24 hrs with supernatants from MLR cultures in Fig. 3. Fibroblast RNA was prepared and expression of selected genes measured with Nanostring. (A) PLSDA was applied to Nanostring data and plot shows LV1 for gene expression data of fibroblasts exposed to supernatants from each anti-co-IR antibody-treated MLR. Data points represent values for each individual healthy and SSc donor. (B) Bar graph shows the contribution of individual genes to LV1. Asterisks designate genes that contributed most to LV1 separation of anti-TIM-3-mediated changes, as calculated by VIP score.

Table 1

Clinical Features of Systemic Sclerosis Patients and Healthy Controls

Characteristic	HC	SSc
	n=19	n=28
Sex, number males/females	8/11	1/27
Age	52 (25–69)	57 (32–68)
Age of Onset, median	NA	46 (24–74)
Disease Duration	NA	7.3 years (1 month – 42 years)
Race, Hispanic-White/Black/White	0/1/18	2/0/26
Number dSSc/lSSc	NA	6/22
Modified Rodnan Skin Score	NA	5 (0–36)*
Lungs		
ILD	NA	9
PAH	NA	10

*7 patients no MRSS reported